

# The Effect of Electropolishing on the Surface Topography of Direct Machined Simulated Coil Gaps

ICOMM  
2012  
No.

Lysle M. Serna<sup>1</sup>, Bradley H. Jared<sup>2</sup>, Brad L. Boyce<sup>3</sup> and Gerald A. Knorovsky

Science and Engineering Center, Sandia National Laboratories, USA

<sup>1</sup>e-mail: [lmserna@sandia.gov](mailto:lmserna@sandia.gov); <sup>2</sup>e-mail: [bhjared@sandia.gov](mailto:bhjared@sandia.gov);

<sup>3</sup>[blboyce@sandia.gov](mailto:blboyce@sandia.gov)

## INTRODUCTION

State of the art machining technologies, such as pulse laser and micro-wire electrodischarge machining ( $\mu$ -WEDM), have allowed miniaturization of mechanical devices to be realized. Using these precision machining tools, small dimensional tolerances (about an order of magnitude greater than silicon micromachining) can be achieved. Because of a lack of alternatives, miniature conventional (coil wound) springs are still used in small mechanism applications, despite exhibiting large manufacturing uncertainties (e.g. bend radius and tang orientation) that result in design tolerances of  $\pm 20\%$  or more. Miniature coil wound springs are those with wire diameters smaller than 100  $\mu\text{m}$ . The large design margins required for coil springs can produce an unfavorable cascade effect in design parameters, resulting in an increased mechanism size, and are therefore detrimental to the effort to miniaturize.

One possible alternative to coil wound springs are springs direct machined from bar stock, tube, sheet, and other forms. Machined helical springs of a wide range of sizes are commercially available [1]. As currently reported, the minimum slot size (gap between coils) for a machined extension spring is approximately 0.020 inch (0.51 mm) [2]. In contrast, at the *microscale*, 4 micron wide “micro-machined” thin film MoCr springs with 1 to 2 micron slots have fabricated for use in vertical-cavity surface-emitting laser (VCSEL) arrays [3].

Precision machining on the mesoscale bridges the gap between macro and micro-scale manufacturing processes, and can achieve dimensional tolerances on the order of one micron. Femtosecond laser machining and  $\mu$ -WEDM each have the high accuracy, resolution, and minimal material impacts required for the fabrication of structural spring features. Mesoscale springs present a promising alternative if they are proven to provide improved repeatability, manufacturability, and reliability over coil springs of the same overall dimension.

The surface characteristics, e.g. roughness, of engineered surfaces have a significant effect on in-service material performance, and can be directly related to device performance and reliability, particularly for small mechanisms. Ironically, one disadvantage of precision machining is the relatively poor surface finish compared to that required for most precision applications. Femtosecond laser machining and  $\mu$ -WEDM are inherently thermally driven processes in which metal is removed by highly localized metal vaporization, melting and re-solidification to produce a characteristic sur-

face morphology and topography.  $\mu$ -WEDM removes material by high repetition electrical discharges from a wire to the sample through a dielectric medium, which is typically oil or water. The dielectric also serves to flush debris from the cut surface and effectively quenches the melted surface layer. The result is a “recast” layer of re-solidified material on the cut surface, which can be minimized by optimizing process parameters, and performing “trim” passes, but cannot be eliminated. Fig. 1 is a scanning electron micrograph showing a representative recast layer topography for  $\mu$ -WEDMed 304L stainless steel. This surface layer is brittle in nature and thus highly susceptible to micro-cracking induced by residual tensile stresses from the rapid re-solidification process. Micro-cracks are often observed in the recast layer for traditional EDMed parts [4,5], and are believed to be similarly present in  $\mu$ -WEDMed surfaces, although more difficult to detect. Of particular relevance for spring performance, the recast layer adversely affects fatigue resistance [6]. Consequently, removal of recast is required in order to improve material performance.

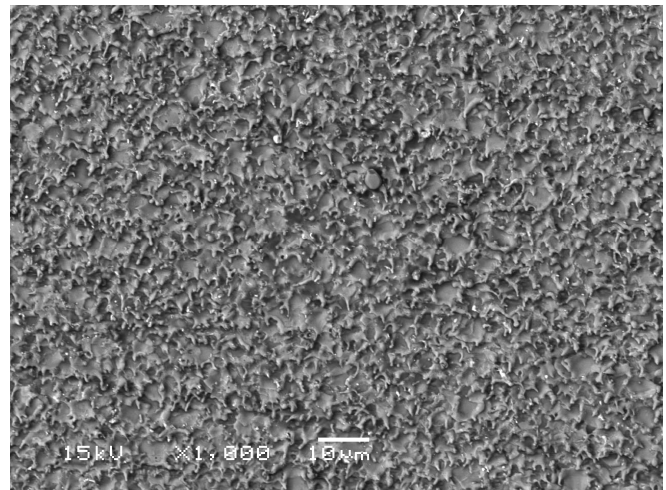
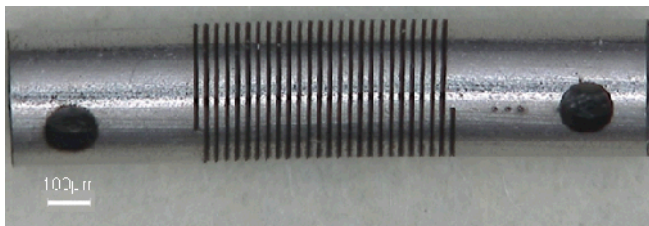


Fig. 1: Scanning electron micrograph of  $\mu$ -WEDM recast layer on 304L stainless steel.

Electropolishing is a commonly used technique that improves surface finish by making the metal item of interest an anode in a concentrated acid electrolyte [7,8]. In the course of electropolishing, the current density over the surface of the metal varies from site to site, largely depending on the anode to cathode distance. Surface asperities will have higher current densities compared to recessed areas, resulting in preferential dissolution of the asperities, and a smooth surface. Electropolishing has been shown to improve the corrosion resistance

and coating adhesion of biomedical implant materials such as 316 stainless steel [9,10]. In addition to improving corrosion resistance and coating adhesion, electropolishing can also improve mechanical properties such as fatigue resistance in aluminum and steel test coupons by removing the recast layer to produce smooth, almost featureless, surface that is free of residual tensile stress [11].

Recently, precision direct machining has been used to fabricate *mesoscale* springs [12]. Due to its ideal dimensions for this application (i.e. small outer diameter and thin wall thickness), and commercial availability, hypodermic needle tubing is used as the starting form for machining mesoscale springs. Fig. 2 shows an example of a mesoscale spring fabricated by precision machining.



**Fig. 2: Optical micrograph of mesoscale spring machined from 304L stainless steel hypodermic needle.**

In this work, the effect of electropolishing on surface topography of  $\mu$ -WEDMed simulated coil surfaces was investigated by scanning electron microscopy (SEM) and atomic force microscopy (AFM). In addition to reducing surface roughness, electropolishing is also effective at removing embedded particle contamination from the EDM micro-wire. It is important to note that electropolishing works very well for simple geometries in which the target surfaces (the anode) are boldly exposed and have a direct line of sight to the cathode. Material within coil gaps such as those shown in Fig. 2 present a challenge for electropolishing due to the non-ideal anode to cathode orientation.

## EXPERIMENTAL PROCEDURES

Samples for electropolishing were fabricated using commercially available 304L (18Cr-8Ni-balance Fe) stainless steel hypodermic needle tubing. The tube material was received in the  $\frac{3}{4}$  to full hard cold worked condition.

Simulated coil gaps were machined into the tubing using an Agie Vertex 1F  $\mu$ -WEDM machine. Fig. 3 shows an (a.) schematic representation and (b.) scanning electron micrograph of a segment of an electropolishing test sample with a simulated coil gap. A small tab of material was left at the base of the gap so that the sample could be kept intact during handling and electropolishing and then purposely broken open to evaluate the resulting topography of the gap surfaces. The tab size was optimized in the following way: 1) minimized so that solution flow in the gap area was not that excessively perturbed and 2) sufficient in size to provide me-

chanical stability to the sample to allow manual handling. Simulated coils gaps of 40, 60, 80 and 100  $\mu$ m were fabricated in order to investigate the effect of gap width on electropolishing effectiveness (i.e. ability of electropolishing to remove the recast layer from the outer to the inner edge of the coil).

The Agie 1F processing parameters are proprietary “technologies” not known to the authors, other than the use of an AC pulse generating circuit. Samples were  $\mu$ -WEDMed using a 20  $\mu$ m tungsten wire and deionized water as the dielectric and flushing medium. Wire gap distances of 13-15  $\mu$ m for the main pass and 10-12  $\mu$ m for the trim pass were used. The trim pass significantly reduced the amount of recast on the surface. Fig. 4 is an scanning micrograph showing a representative recast layer after (a.) the main pass and (b.) trim pass.

Electropolishing was performed using a BK Precision Model 9121A power supply. The anode and cathode used in the electrolytic cell are the 304L electropolishing sample and a platinized Nb mesh, respectively. Samples were electropolished in an electrolyte typically used for stainless steels consisting of 80vol%  $H_3PO_4$  + 20vol% n-butanol [13]. The electrolyte temperature was maintained at  $70^\circ C \pm 5^\circ C$ . An initial study was performed to investigate the effect of electrolyte stir rate on electropolished surface topography of the gap surface. Stir rates of 300, 400, and 500 rpm were evaluated. Results indicated no improvement in surface finish for increased stir rates, therefore 300 rpm as used for the remainder of the experiments. Based on prior experience, electropolishing was performed using a current density of 350 mA/cm<sup>2</sup>. For this work, the effect of electropolishing for immersion times of 1, 2 and 3 minutes on the surface morphology and topography of the 40 m and 100m gap are presented.

Surface roughness was measured by Atomic Force Microscopy (AFM) using a Veeco Dimension Icon AFM with a TESPA tip and operating in 0.4 Hz Peakforce Tapping Mode. Three dimensional scans were collected over a scan area of 20 x 20  $\mu$ m (512 x 512 pixels).

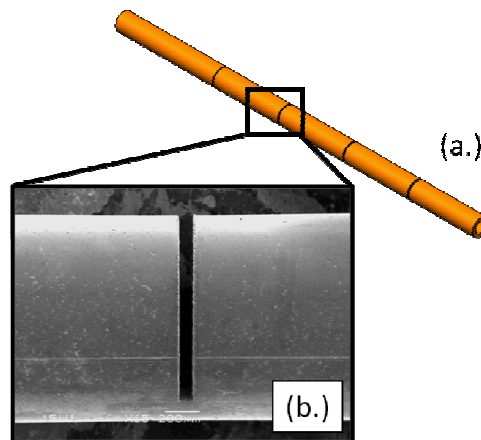


**Fig. 3: (a.) Schematic of electropolishing sample and (b.) scanning electron micrograph of simulated coil gap.**

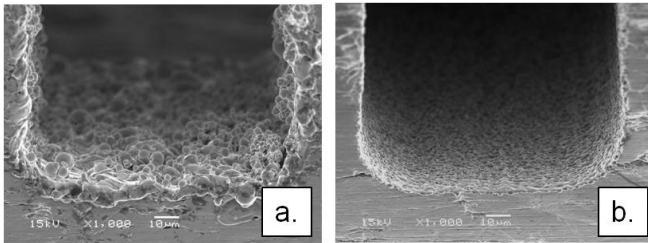


Fig. 4: Scanning electron micrograph of base of simulated coil gap (a.) after  $\mu$ -WEDMed main pass and (b.) trim pass.

## RESULTS

To provide a baseline for the electropolished samples, the surface topography of the  $\mu$ -WEDMed surfaces was examined by SEM and measured by atomic force microscopy (AFM). Fig 5 shows a scanning electron micrograph of a representative surface for a 40 micron gap surface in the as machined condition. The fracture surface of the tab can be seen on the right side of the tube. The  $\mu$ -WEDMed machining process results in two distinct surface topographies. In Fig 5, a repeating pattern of striations that appears to follow the cutting direction across the tube. AFM data indicate that the peak-to-valley height difference of these ridge and valley-like features is on the order of 2  $\mu$ m.

Fig 6 shows (a.) a scanning electron micrograph of a  $\mu$ -WEDMed simulated coil gap surface and (b.) 3-D AFM micrograph for a 20 x 20 micron scan of a similar area. As discussed previously, the surface topography of EDMed surfaces is characterized by a uniform distribution of nodule-like asperities that formed during local re-solidification of the cut metal. The AFM measured arithmetic mean surface roughness ( $R_a$ ) and peak roughness ( $R_{max}$ ) for  $\mu$ -WEDMed surfaces are summarized in Table 1. The overall average measured surface roughness ( $R_a$ ) for the  $\mu$ -WEDMed surfaces is  $272 \pm 31$  nm (average of 24 measurements; 6 per gap surface). There was no statistically significant variation in surface roughness as a function of gap width.

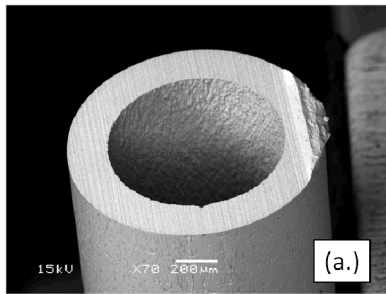


Fig. 5: Scanning electron micrograph of  $\mu$ -WEDMed simulated coil gap surface.

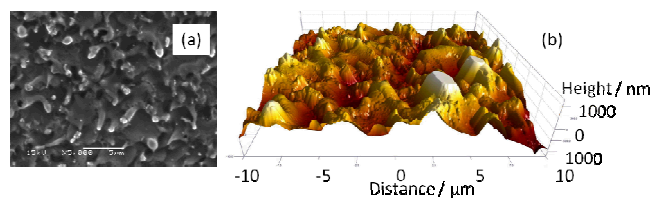


Fig. 6: (a.) Scanning electron micrograph of  $\mu$ -WEDMed simulated coil gap surface and (b.) 3-D AFM micrograph for a 20 X 20 micron scan of a similar area.

Table 1: AFM measure surface roughness for  $\mu$ -WEDMed surfaces. All units in nm.

	Average $R_a$	Std Dev	$R_{max}$ (Z range)	Std Dev
40 micron	257	27	1926	220
60 micron	269	33	2099	223
80 micron	277	28	2222	443
100 micron	286	36	2284	266
Overall	272	31	2082	314

Fig 7. shows a series of backscatter electron scanning electron micrographs for a 40 micron (top row) and 100 micron (bottom row) gap surfaces electropolished at 350 mA/cm<sup>2</sup> for immersion times of 1, 2 and 3 minutes (shown from left to right). In each of these micrographs, the outer tube diameter is on the left (with the exception of Fig 7f, in which the outer tube wall is on the right). One minute is clearly insufficient immersion time to remove the recast layer from the gap surface, independent of gap width (Fig 7a and d). By increasing the polishing time to 2 minutes, we start to see the effects of electropolishing at the outer tube edges, which appears smooth compared to the inner edge of the tube. At 2 minutes, the 100 micron gap surface appears to be more polished compared to the 40 micron gap, although in each case, the machining striations are still apparent. For the 40 micron gap surface, 3 minutes of polishing time results in additional smoothing of the outer tube edge, with a minimal apparent effect on the surface topography of the inner edge. In contrast, at 3 minutes polishing time, the 100 micron gap surface is completely smooth, with no visible asperities or striations.

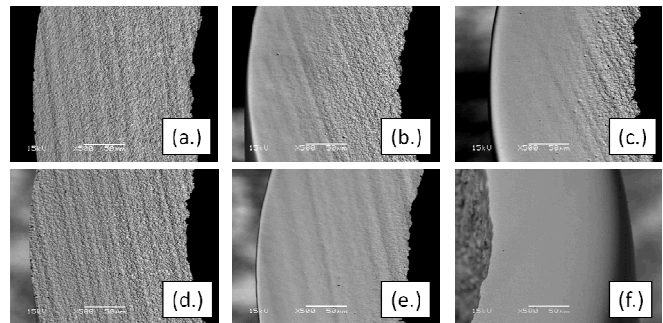


Fig. 7: Backscatter electron SEM micrographs for electropolished gap surfaces (gap width, polishing time). (a.) 40  $\mu$ m, 1 minute, (b.) 40  $\mu$ m, 2 minutes, (c.) 40  $\mu$ m, 3 minutes, (d.) 100  $\mu$ m, 1 minute, (e.) 100  $\mu$ m, 2 minutes, and (f.) 100  $\mu$ m, 3 minutes.

The AFM measured surface roughness ( $R_a$ ) for electropolished surfaces are summarized in Table 2. For conciseness, only surface roughness for the minimum (40 micron) and maximum (100 micron) gap surfaces electropolished for 3 minutes is reported. In order to quantify electropolishing effectiveness, surface roughness was measured for areas closest to the outside and inside edges of the tube surface. For the 40 micron gap surface, electropolishing at 300 mA and 3 minutes reduced the  $R_a$  from 257 nm to 100 nm, a reduction of over 50%. The reduction in surface roughness is more dramatic at the outside edge of the same sample.  $R_a$  at the outside edge is 16 nm, an over 90% reduction in surface roughness. Increasing the gap width to 100  $\mu\text{m}$  eliminates the variation in surface roughness across the electropolished gap surface. The  $R_a$  for the outside and inside edges of the 100 micron gap surface is very similar at 19 nm and 22 nm, respectively, again representing a >90% reduction in surface roughness.

**Table 2: AFM measure surface roughness for electropolished (3 minutes) gap surfaces. All units in nm.**

	Outside edge		Inside edge	
	Average		Average	
	$R_a$	Std Dev	$R_a$	Std Dev
40 micron	16	12	100	50
100 micron	19	4	22	8

Fig 8 shows a 3-D AFM micrograph for a 20 x 20 micron scan of an electropolished area on a 100 micron gap surface. The effectiveness of electropolishing at removing both fine asperities and machining striations to produce a smooth surface is readily apparent.

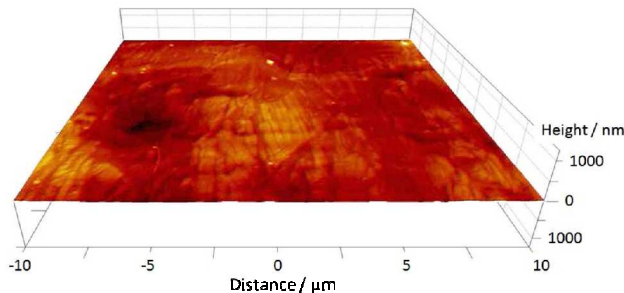


**Fig. 8: 3-D AFM micrograph (20 X 20 micron scan) of  $\mu$ -WEDMed and electropolished (3 minutes) surface of a 100 micron gap surface.**

spring fatigue life.

## ACKNOWLEDGMENTS

Sandia National Laboratories is a multi-program laboratory managed and operated by Sandia Corporation, a wholly owned subsidiary of Lockheed Martin Corporation, for the U.S. Department of Energy's National Nuclear Security Administration under contract DE-AC04-94AL85000. This document has been reviewed and approved for unclassified, unlimited release under **SAND2011-6912A**.

## REFERENCES

- [1] Helical Products Company, Inc., Santa Maria CA, 93456-1069.
- [2] G.L. Boehm, "Which Spring to Choose: Coiled Wire vs. Machined, a Comparison", *Mechanical Engineering*, web exclusive, August 2010. [http://memagazine.asme.org/web/Which\\_Spring\\_Choose\\_Coiled.cfm](http://memagazine.asme.org/web/Which_Spring_Choose_Coiled.cfm)
- [3] C. L.Chua, D.K. Fork, D. L. Smith, and H. McIntyre, "High Density Packaging of Vertical-Cavity Surface-Emitting Laser Arrays using Micro-machined Springs," *Lasers and Electro-Optics Society, 13<sup>th</sup> Annual Meeting*, 2000, IEEE.
- [4] L.C. Le, L.C. Lim, V. Narayanan, and V.C. Venkatesh, "Quantification of Surface Damage of Tool Steels After EDM", *Int. J. Mach. Tools Manufact.*, 1988; Vol. 28, No.4:359-372.
- [5] L.C. Lee, L.C. Lim and Y.S. Wong, "Crack susceptibility of electro-discharged machined surfaces," *J. Materials Processing Technology*, 1992; Vol 29: 213-221.
- [6] R.D. Rhew, "A Fatigue Study of Electrical Discharge Machine (EDM) Strain-Gage Balance Materials," *International Congress on Instrumentation in Aerospace Simulation Facilities (ICIASF)*, 1989, 477-487.
- [7] ASTM E1558, "Standard Guide for Electrolytic Polishing of Metallographic Specimens," 2009.
- [8] D. Landolt, "Review Article Fundamental Aspects of Electropolishing," *Electrochimica Acta*, 1987; Vol. 32, No.1: 1-11.
- [9] E. J. Sutow, "The influence of electropolishing on the corrosion resistance of 316L stainless steel," *J. Biomedical Materials Research*, 1980; Vol.14: 587-595.
- [10] M. Haidopoulos, S. Turgeon, G. Laroche, D. Mantovani, "Surface modifications of 316 stainless steel for the improvement of its interface properties with RFGD-deposited fluorocarbon coating," *Surface & Coatings Technology*, 2005; 197:278-287.
- [11] S. Jeelani and M.A. Scott, "How surface damage removal affects fatigue life," *Int. J. Fatigue*, 1988; Volume 10 No 4 : 257-260.
- [12] B.H. Jared et al., "Design and Fabrication of Direct Machined Mesoscale Springs," *ICoMM*, 2012.
- P. Dettner, "Electrolytic and Chemical Polishing of Metals", *Orderlich Publishers*, 1988.

## CONCLUSIONS

The effectiveness of electropolishing simulated coil gaps ranging from 40 to 100  $\mu\text{m}$  in 304L hypodermic tubing has been demonstrated. The resulting topography was found to be dependent on electropolishing time and gap width. A uniformly smooth surface was achieved for a 100  $\mu\text{m}$  gap electropolished for 3 minutes at 350 mA/cm<sup>2</sup>. Future work will focus on electropolishing of actual mesoscale extension springs and determining the effect of electropolishing on